ELSEVIER

Journal of Power Sources 79 (1999) 9–18

JOURNAL OF POWER SOURCES

Synthesis, characterization and application of doped electrolytic manganese dioxides

Wolfgang Jantscher, Leo Binder *, Dirk A. Fiedler, Reinhard Andreaus, Karl Kordesch

Institut für Chemische Technologie Anorganischer Stoffe, Technische Universität Graz, Stremayrgasse 16 / III, A-8010 Graz, Austria

Received 14 May 1998; received in revised form 24 August 1998; accepted 5 September 1998

Abstract

Electrolytic manganese dioxides (EMDs) were prepared on the 100 g scale by anodic deposition from acidic aqueous solutions of manganese sulfate. In situ doping with titanium ions was achieved by addition of tetra-*n*-butoxytitanium to the electrolytic bath. Samples were also doped ex situ by washing the products with aqueous barium hydroxide solution. The EMDs were characterized by electron microscopy studies and BET surface area determinations. Cyclic abrasive stripping voltammetry was successfully applied to evaluate the rechargeability of the newly synthesized undoped and doped EMDs in 9 M KOH. Relative discharge capacities at different depths of discharge (DOD) with respect to the first one-electron reduction of γ-MnO_2 are compared for different EMDs. At about 30% DOD, resulting relative discharge capacities show essentially the same trend as those measured in AA cells from about 10 to 20 discharge/charge cycles onwards. Accordingly, titanium-doped EMD was shown to exhibit superior charge retention and rechargeability when compared to the titanium-free samples.

Keywords: Electrolytic manganese dioxide; Rechargeable alkaline batteries; Abrasive stripping voltammetry; Rapid cycling; Electron microscopy; Doping; Titanium; Barium

1. Introduction

Electrolytic manganese dioxide (EMD) is used as a major compound of the composite cathode in rechargeable alkaline manganese dioxide (RAM™) cells. The rechargeability of these batteries depends on the partial discharge of the manganese dioxide cathode to avoid problems associated with manganese dioxide deep discharge. The applied depth of discharge (DOD) is a determining factor for the cycle life (number of charge/recharge cycles) of these RAM cells. Many attempts have been made to improve the cycle life at increasing DOD of the manganese dioxide cathode [1]. At an early stage of development Ti(IV) was found useful for stabilizing the structure of EMD [2]. As an attempt to improve the rechargeability of RAM™ cells, electrolytically Ti-doped manganese dioxides have been produced [3]. This work will focus on various analytical aspects related to those materials. In particular, the recently developed electroanalytical technique of abrasive stripping voltammetry (AbrSV) [4–7] has been shown to be applicable to meaningful studies in the area of battery electrode material research [3,8–10]. In the following, we compare results from AbrSV experiments on the newly synthesized doped EMDs with those from AA-sized RAM™ cells also containing these cathode materials.

2. Experimental

2.1. Preparation

The synthesis of in situ-doped EMDs under various conditions is described in Ref. [3]. EMD deposits were mechanically removed from the anode and rinsed with deionized water. After neutralization with diluted $Ba(OH)_2$-solution, repeated washing with deionized water and drying, the product was ground and sieved through a 125 μm mesh. The resulting powders from batch nos. 2 (undoped EMD) and 6 (titanium-doped EMD) as described in Ref. [3] were taken for further investigations (cf. Table 1). Considering the washing procedure described above, the initially undoped sample is named EMD:Ba in the

* Corresponding author. Tel.: +43-316-873-8263; Fax: +43-316-873-8272; E-mail: f537bind@mbox.tu-graz.ac.at

0378-7753/99/$ - see front matter
PII: S0378-7753(98)00163-3

Table 1
Selected results from laboratory EMD electrodeposition [3]

Sample	Yield [g]	Current efficiency [%]	Ti content [wt.%]
EMD:Ba[a]	310	98	0
EMD:(Ba, Ti)[b]	200	65	0.63

[a] Batch no. 2 of note [3]; anode: Pb alloyed with 3% Sb.
[b] Batch no. 6 of note [3]; anode: Pb.

following. Analogously, the other sample is abbreviated EMD:(Ba, Ti).

2.2. Characterization

The amount of titanium in the doped EMD sample was determined by a photometric method. A BET surface analyzer (Quantachrome) was used to measure the BET surface area (adsorbate = nitrogen) of different EMDs.

Samples were routinely controlled with a Jeol JSM-35CF scanning electron microscope (SEM). A transmission electron microscope (TEM) was applied for inspection of the titanium-doped EMD. These investigations were performed with a Philips CM20/STEM. The microscope was equipped with a post column imaging filter (GIF by Gatan) which allows the acquisition of energy-filtered images (EFTEM) [11]. The powder was mounted on carbon nets using standard TEM preparation procedures. The distribution of Ti within the specimen was accessible through recording energy-filtered images at the Ti L_{23} ionisation edge. Resulting Ti elemental maps were derived according to the procedure described in Ref. [12].

2.3. Electrochemistry

Electrochemical boundary conditions were exactly as detailed in an earlier contribution [9]. Commercially available γ-MnO_2 (TOSOH Hellas A.I.C., Greece, ≤ 90 μm) is termed 'reference EMD' in the present work.

For the determination of the amount of MnO_2 being attached to the surface of the 0.5 mm diameter Pt disk electrode, the procedure was also exactly as described in Ref. [9].

2.4. Batteries

AA-sample RAM™ cells were assembled from the initially undoped and titanium-doped EMD samples (EMD:Ba and EMD:(Ba, Ti) laboratory production) as well as from reference EMD. Testing of the different materials was done on a computer-controlled test stand. The cells were discharged across a 3.9 Ω resistor to a discharge cut-off voltage of 900 mV. Voltage-limited taper charging was used to charge cells to 1720 mV.

3. Results and discussion

A number of different results from EMD electrodeposition are described elsewhere [3]. Selected samples which were studied in more detail are briefly recollected in Table 1.

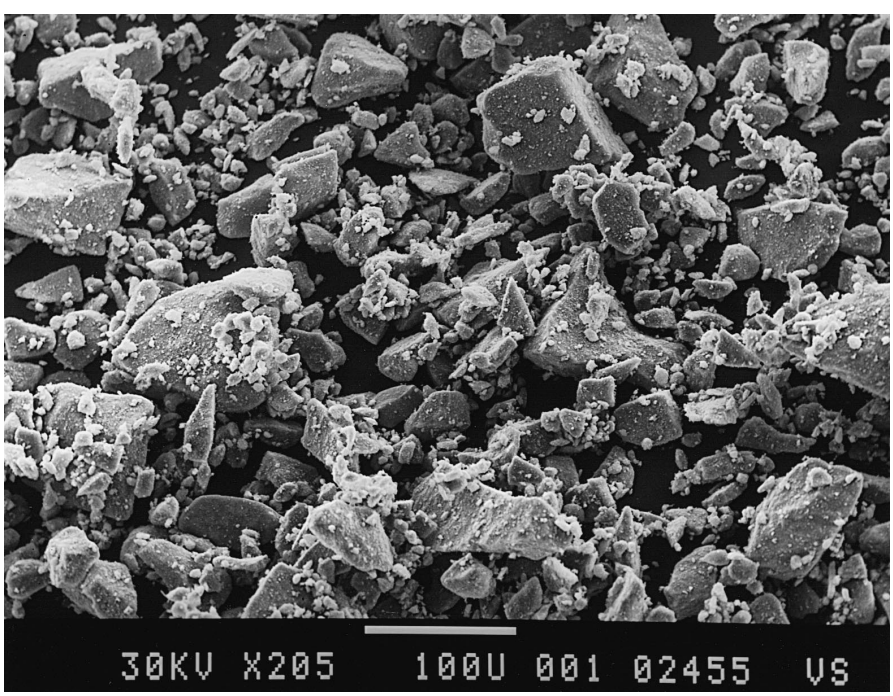

Fig. 1. SEM-image of reference EMD at 205-fold magnification.

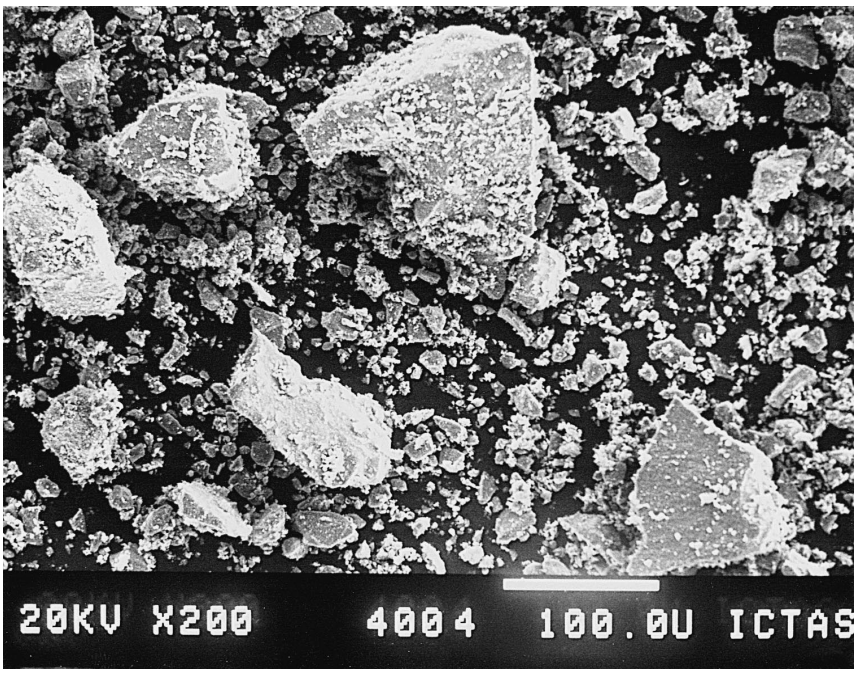

Fig. 2. SEM-image of EMD:Ba at 200-fold magnification.

SEM images of reference EMD, EMD:Ba and EMD:(Ba, Ti) are shown in Figs. 1–3, respectively. Besides the apparently narrower grain size distribution for the reference material, which would be expected for an industrial product, the appearance of the three materials is similar. All EMDs consist of cornered and uneven particles with rough surfaces, which, compared to reference EMD, is typical for the preparation method. No particular difference in apparent hardness was encountered when attaching these materials to the surface of an electrode in abrasive stripping voltammetric experiments discussed below.

The TEM-image in Fig. 4a shows a typical specimen region of the titanium-doped EMD:(Ba, Ti) at higher magnification. The titanium content of the EMD sample is

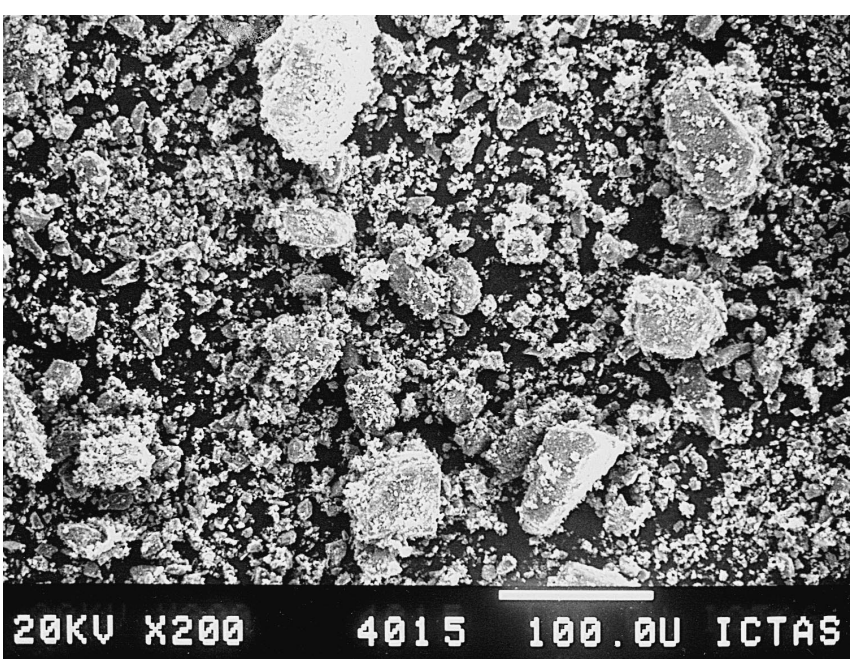

Fig. 3. SEM-image of EMD:(Ba,Ti) at 200-fold magnification.

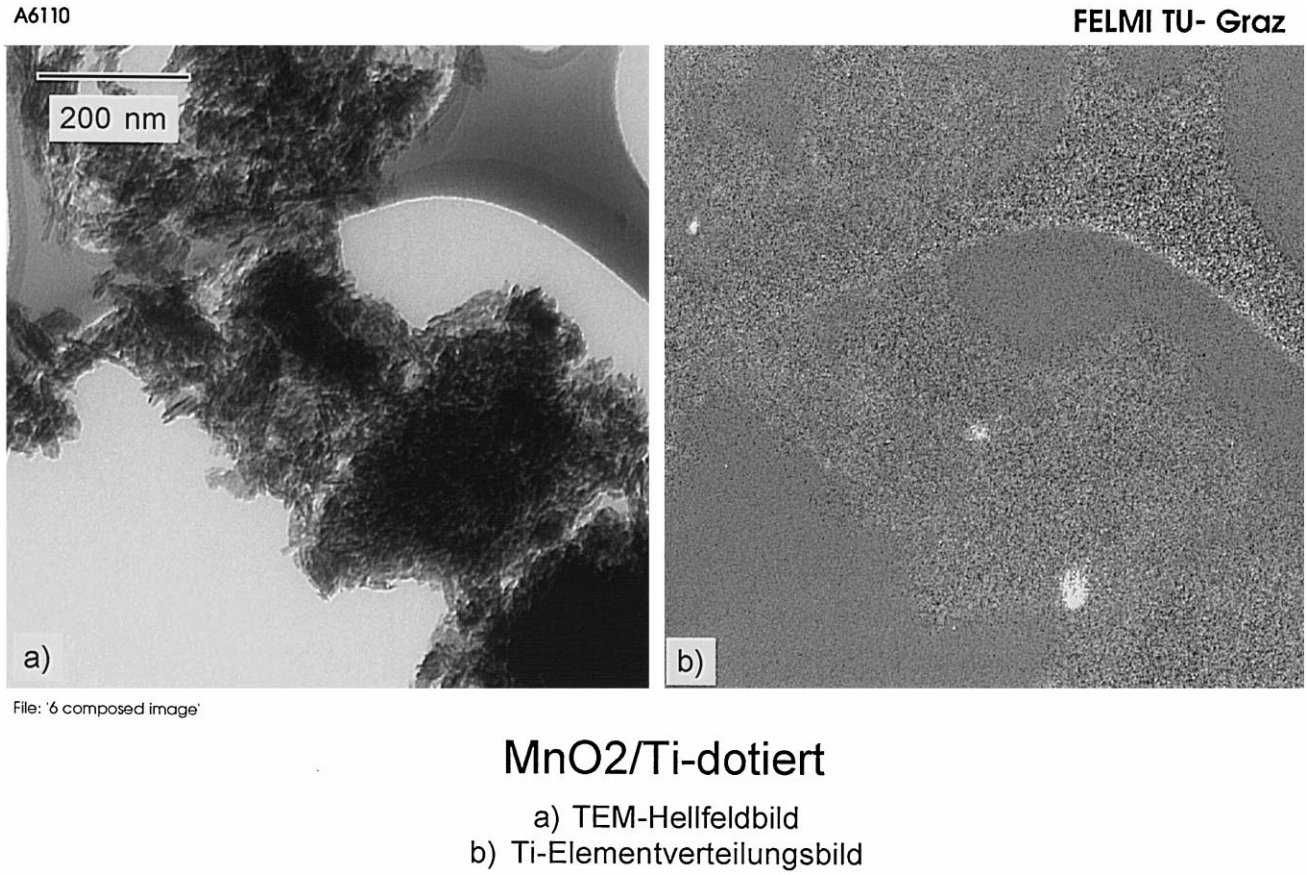

Fig. 4. (a) TEM image of EMD:(Ba,Ti) in bright field detection mode. (b) Resulting Ti elemental map derived from energy-filtered TEM images at the Ti L_{23} ionization edge.

0.63 wt.%. The resulting Ti-elemental map in Fig. 4b indicates by showing a uniformly grey shaded area and barely bright spots that most of the incorporated titanium is homogeneously distributed. Under the experimental conditions the codeposition of doping ions can be explained mainly by adsorption processes [13]. The manganese dioxide surface strongly adsorbs metal ions from the solution by ion exchange with protons of surface hydroxyl groups. The adsorbed metal ions form surface complexes which will be converted to oxides when they are enclosed in the bulk of the growing EMD. The specific (= BET) surface area, S_{Bet}, of EMD:(Ba, Ti) is larger than those for EMD:Ba or reference EMD (Table 2). This may be explained as follows: in connection with the described adsorption process the presence of doping ions results in many structural defects or a large number of smaller EMD particles.

Table 2
Specific surface areas, S_{BET}, and pre-heating conditions for different EMD samples

Sample	Specific surface area [$m^2\ g^{-1}$]	Correlation	Heating conditions
Reference EMD	20.117	0.997	90°C/30 min
EMD:Ba	20.822	0.998	85°C/12 h
EMD:(Ba, Ti)	81.347	0.977	85°C/17 h

Fig. 5 shows the cyclic abrasive stripping voltammetric response of reference EMD in 9 M KOH. Process I, as defined in Eq. (1), is observed in the potential range of 200 to −350 mV [8,14–16], that is, between potentials E_0 and E_1.

$$\text{Process I} \quad \gamma - MnO_2 + H_2O + e^- \rightarrow MnOOH^-_{OH} \qquad (1)$$

$$\text{Process II} \quad MnOOH + H_2O + e^- \rightarrow Mn(OH)_2 + OH^- \qquad (2)$$

Process II is then observed between −350 and −800 mV. A detailed discussion of this reaction mechanism, in the context of AbrSV, is given in Refs. [8,9]. For the purpose of this article, we wish to point out the general similarity of voltammograms of reference EMD in either plain or barium-saturated 9 M KOH and those of both EMD:Ba and EMD:(Ba, Ti), see Figs. 6–8.

The presence of Ba^{2+} ions in the electrolyte solution is known to enhance the rechargeability of EMD [9,17–19]. As will be detailed in a forthcoming report [20,21], formation of barium manganates from γ-MnO_2 is indicated by a shift in peak potential for the signal assigned to process II by about 50 mV. Formation of barium-containing products [9,20,21] appears to take place slowly when looking at reference EMD, Fig. 6, as judged by a shifting peak

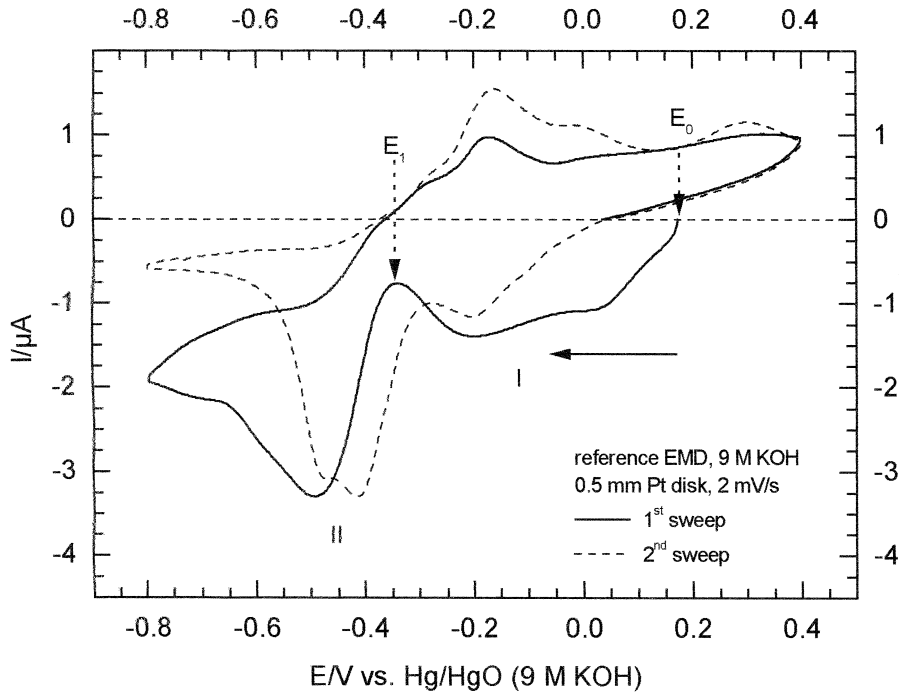

Fig. 5. Cyclic abrasive stripping voltammetry of reference EMD. Scan direction as indicated by solid arrow. Potentials E_0 and E_1 mark integration boundaries as referred to in Section 2.

potential value for process II from −470 to about −420 mV. When EMD is being pre-equilibrated with Ba^{2+} ions by, e.g., washing EMDs with saturated aqueous $Ba(OH)_2$ solution as outlined above, the reduction process II is observed at a peak potential of ca. −420 mV already during the first voltammetric scan, as evidenced for both EMD:Ba and EMD:(Ba, Ti) (Figs. 7 and 8).

As already discussed, barium- and titanium-doped EMD:(Ba, Ti) exhibits about four times the BET surface area when compared to either reference EMD or EMD:Ba (see Table 2). EMD:(Ba, Ti) shows very low reduction and subsequent oxidation currents in voltammetric experiments (Fig. 8a). With roughly the same grain size distribution according to SEM studies (cf. Figs. 1–3), and a signifi-

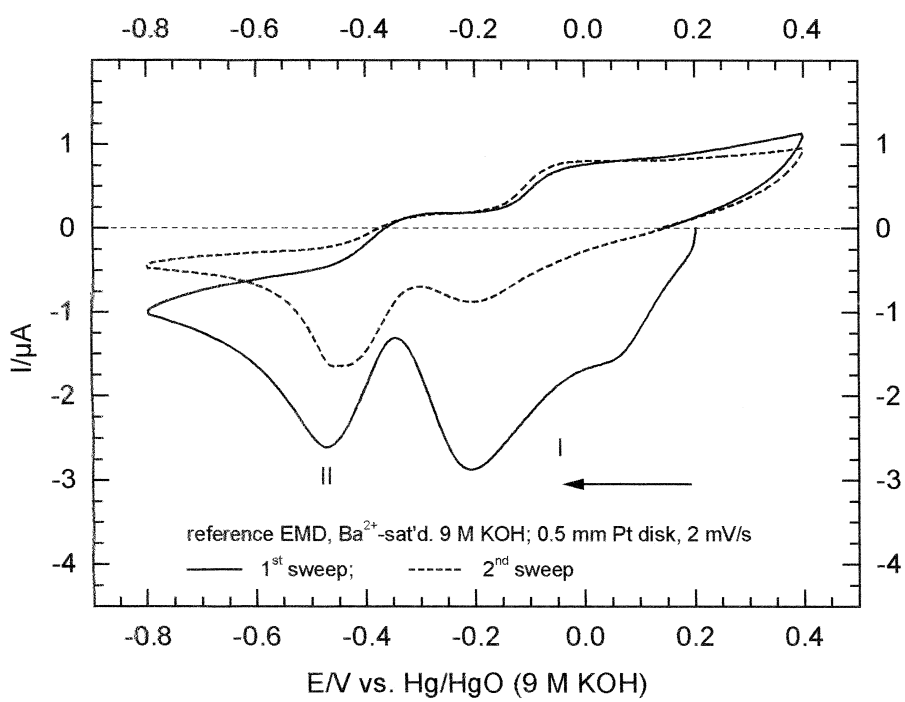

Fig. 6. Cyclic abrasive stripping voltammetry of reference EMD. Scan direction as indicated by solid arrow.

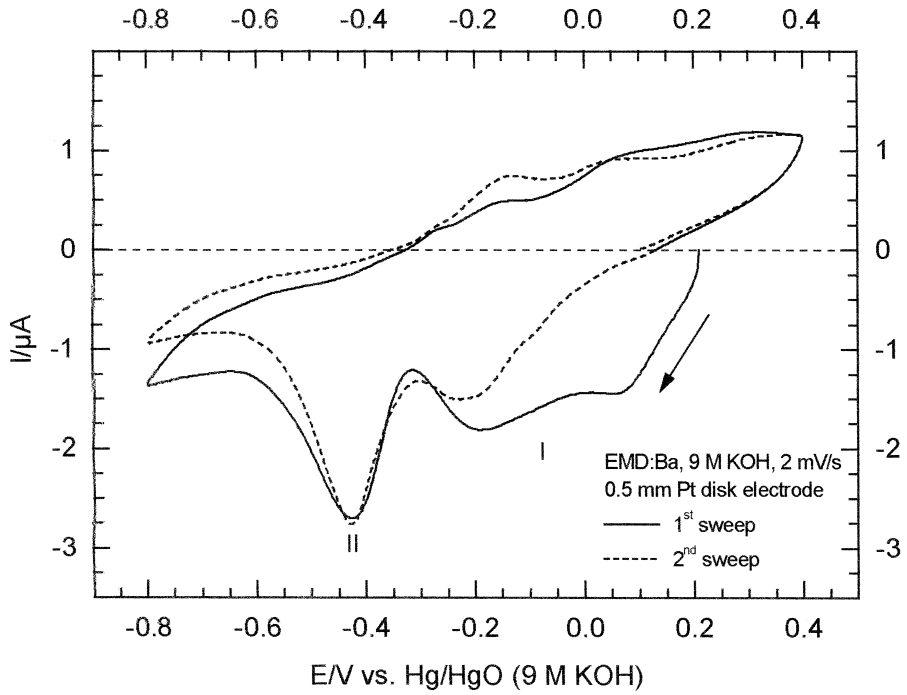

Fig. 7. Cyclic abrasive stripping voltammetry of EMD:Ba. Scan direction as indicated by solid arrow.

cantly larger surface area, one would have expected an increased current response relative to the other two materials. However, we think that EMD:(Ba, Ti) has a fairly high internal resistance because of the increased surface area of the generally poorly conductive material γ-MnO_2, thus preventing an efficient current flow in this experimental setup. This is supported by a comparison of electrochemical and ICP analytical data of different samples of EMD:(Ba, Ti) when attached to the surface of a Pt electrode (see Table 3). Values for used fractions of available EMD:(Ba, Ti) are considerably lower than those for EMD:Ba or reference EMD [9].

When considering abrasive stripping voltammetric data of different experiments on EMD:(Ba, Ti), more peculiarities are observed. In the authors' experience, this is the first EMD whose voltammetric response depends very strongly on the amount of material attached to the electrode as judged by resulting peak currents. Fig. 8b shows the voltammetry when less EMD:(Ba, Ti) adheres to the electrode than in case of the experiment shown in Fig. 8a. Clearly, the first reduction process is dominant, differently structured than before, and the second reduction process is greatly suppressed. We interpret the observed behaviour in terms of dissolution/diffusion processes in the presence of an excess of electrolyte solution. At low electrode loadings, generated manganates-(III) are dissolved and diffuse away from the electrode, resulting in a significant loss of material due to such dissolution reactions on the experimental time scale, effectively reducing the measured reduction currents for processes I and II. At higher loadings, dissolved manganates-(III) are being trapped between the particles adhering to the electrode surface, and are thus accessible for subsequent reduction reactions. Again, due to the barium content of EMD:(Ba, Ti), essentially equal voltammetric behaviour was found in Ba^{2+}-saturated 9 M KOH.

A more significant test of EMDs with respect to the application in, e.g., rechargeable alkaline manganese dioxide cells, is to apply a number of consecutive voltammetric cycles within pre-determined switching potentials as detailed elsewhere [9]. Briefly, the method relies on the integration of the abrasive stripping voltammetric current response over time. For boundary values cf. Fig. 5. When integrating the current over time between $t(E_0)$, $E_0 = 170$ mV, and $t(E_1)$, $E_1 = -350$ mV, we can define a charge value for full one-electron discharge under potentiodynamic conditions. Typical resulting values are in the range of -70 to -300 μA s, which corresponds to the reduction of 0.7 to 3.0 nmol or 63 to 270 ng of γ-MnO_2 according to Faraday's law. The measured open circuit potential is understood to be a mixed potential. With the technique employed here, particles are mechanically attached to the surface of a Pt electrode. Hence, an unknown yet small fraction of the electrode's surface is exposed to the electrolyte solution. Consequently, the observed open circuit potential is a mixed potential, being created by contributions of both Pt and EMD. Results from such integrations are compared with ICP analytical data in Table 3 for two independent measurements each on EMD:Ba and EMD:(Ba, Ti). The different samples of γ-MnO_2 were dissolved after having recorded a full voltammetric cycle encompassing both reduction processes

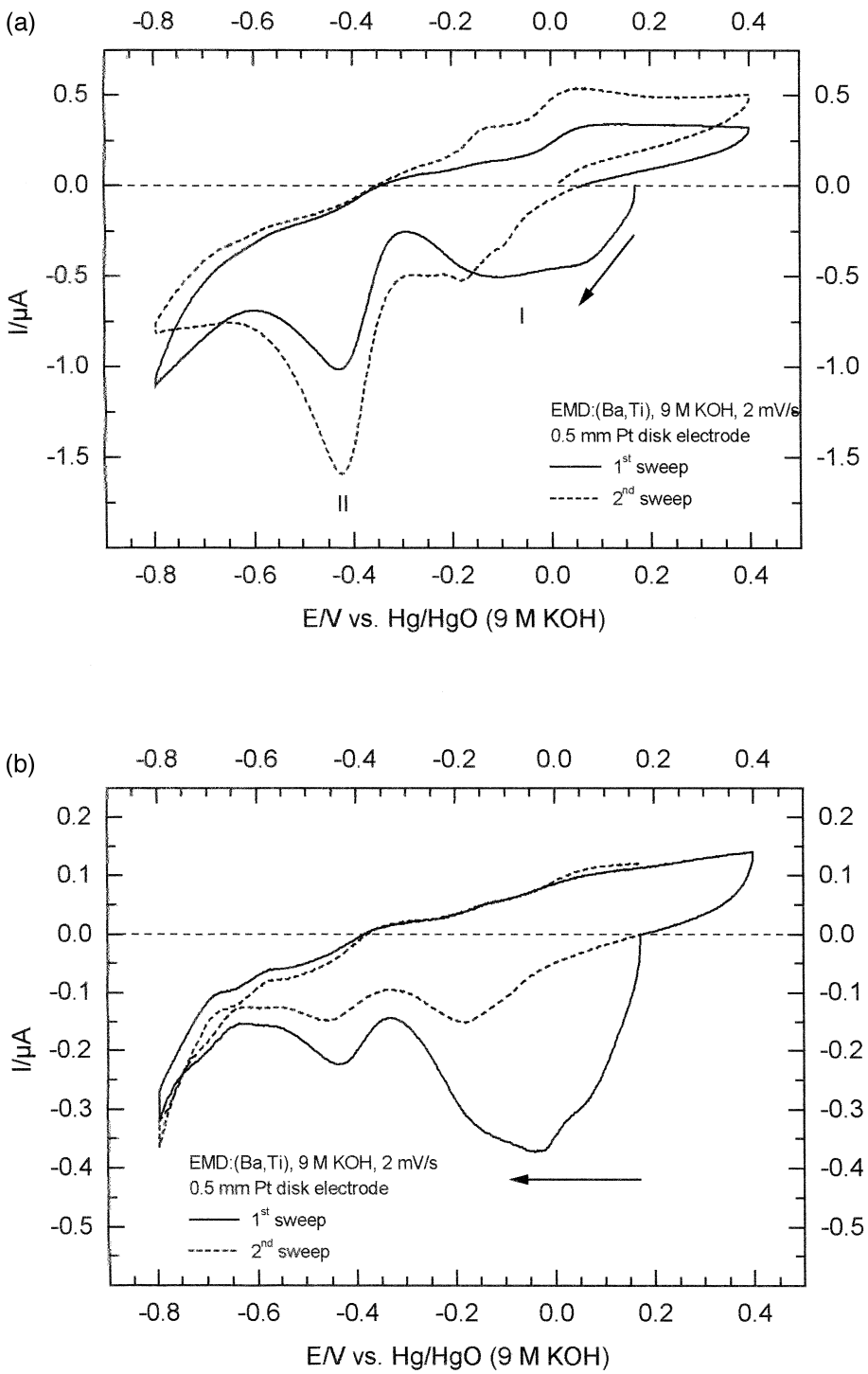

Fig. 8. Cyclic abrasive stripping voltammograms of EMD:(Ba,Ti). Scan direction as indicated by solid arrow. (a) High electrode loading. (b) Low electrode loading.

I and II and subsequent oxidation processes which lead to solid re-oxidized products of type MnO_2 as outlined above. In case of EMD:(Ba, Ti), care was taken to attach sufficient amounts of sample to the electrode surface in order to disable the dissolution/diffusion step observed at low loadings, see above. According to the measured data displayed in Table 3, similar amounts of either EMD were attached to the electrodes. Therefore, irreversible loss of material due to dissolution of products is assumed to have been negligible on the voltammetric time scale. As a result from these ICP determinations, between 2 and 10% of the γ-MnO_2 attached to the electrode are voltammetrically accessible. This gives an idea of material usage in this specific case that can be related to the generally poor

Table 3
ICP-analytical data of dissolved EMDs which were attached to the surface of a 0.5 mm diameter Pt disk electrode and subjected to one voltammetric cycle between −800 and 400 mV prior to dissolution in HCl and dilution to 2.0 ml. Data shown is that of two independent AbrSV experiments on each EMD:Ba and EMD:(Ba, Ti)

EMD, exp. #	$c(\mathrm{Mn})_{\mathrm{corr}}$ [μg l^{-1}][a]	$M(\mathrm{MnO_2})_{\mathrm{corr}}$ [μg][b]	$-Q_{\mathrm{CV}}$ [μA s]	$-Q_{\mathrm{CV}}/M(\mathrm{MnO_2})_{\mathrm{corr}}$ [mA h g^{-1}]	Fraction [%][c]
EMD:Ba #1	725	2.29	260	31.5	10.2
EMD:Ba #2	885	2.80	267	26.5	8.60
EMD:(Ba,Ti) #1	985	3.12	74.4	6.65	2.16
EMD:(Ba,Ti) #2	820	2.60	89.7	9.58	3.11

[a]All measured values are corrected by a value of 15 μg l^{-1} for a blank solution.
[b]Resulting absolute masses of EMDs dissolved in 2.0 ml of sample solution.
[c]Relative to theoretical value of 308 mA h g^{-1} for the one-electron reduction of MnO_2.
Charge values $-Q_{\mathrm{CV}}$ were calculated from the voltammograms by integrating the current response over time in an interval enclosed by E_0 and $E_1 = -350$ mV.

conductivity of γ-MnO_2 [22], and especially EMD:(Ba, Ti). Specific discharge capacities are of the order of 6 to 30 mA h g^{-1}. Such values from AbrSV measurements are comparable with those of high-rate alkaline manganese dioxide battery discharge tests [18] where also only a fraction of the available γ-MnO_2 is discharged [18,22].

Partial reduction or discharge is accordingly defined by switching the potential anywhere between the rest potential and that resembling total one-electron discharge under conditions of AbrSV. By dividing the charge value of partial reduction or discharge by that of complete discharge, we can calculate the depth of discharge (DOD). For a detailed description and discussion of the applied procedure see Ref. [9]. Resulting graphs are displayed in Figs. 9 and 10 for 30% DOD (small, open symbols), corresponding to a potential range of −2 to 400 mV for both EMD:Ba and EMD:(Ba, Ti). The time scale for such experiments is typically 2.7 h, and is a function of the chosen switching potentials at a voltammetric scan rate of 2 mV s^{-1}. The applied boundary conditions, as regards DOD and scan rate, have previously been found to be favourable in the case of a similar type of γ-MnO_2, namely reference EMD [9].

EMD:Ba shows practically the same relative discharge capacity decay in either Ba^{2+}-saturated or plain 9 M KOH, as expected from the cyclic voltammetric data discussed above. The reason for the slightly lower discharge capacities in the presence of Ba^{2+} ions is believed to be formation of pore-blocking $BaCO_3$ during storage under ambient conditions. In plain KOH, some solubility of $BaCO_3$ would

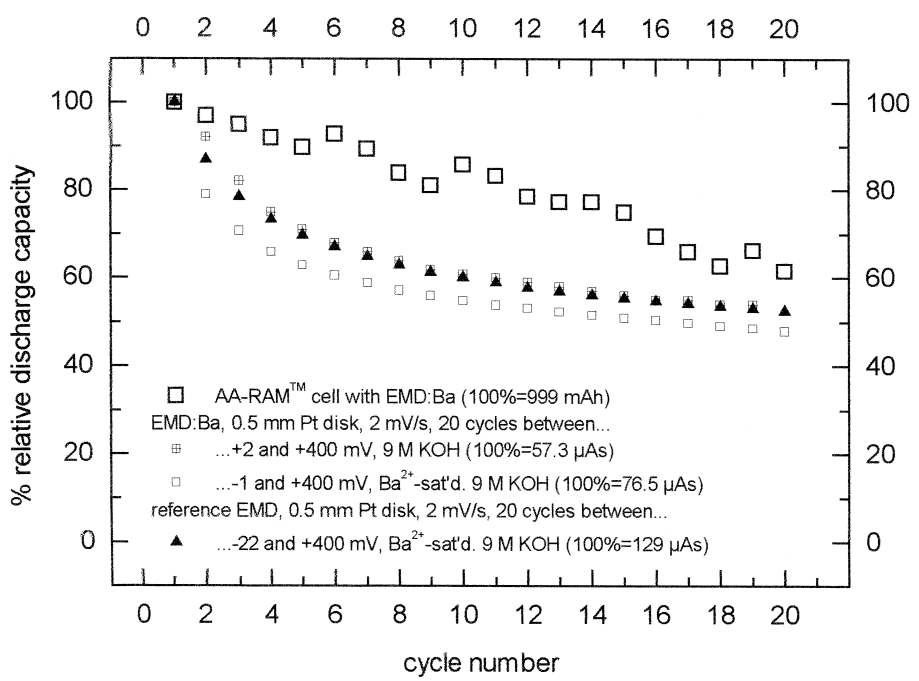

Fig. 9. Relative discharge capacities of reference EMD and EMD:Ba under conditions of AbrSV at 30% DOD. Values corresponding to each 100% discharge capacity are shown. Comparison with data for AA-sized cells which were derived from cycles where the cell was discharged across a 3.9 Ω resistor to 900 mV and subsequently voltage-limited taper charged to 1720 mV.

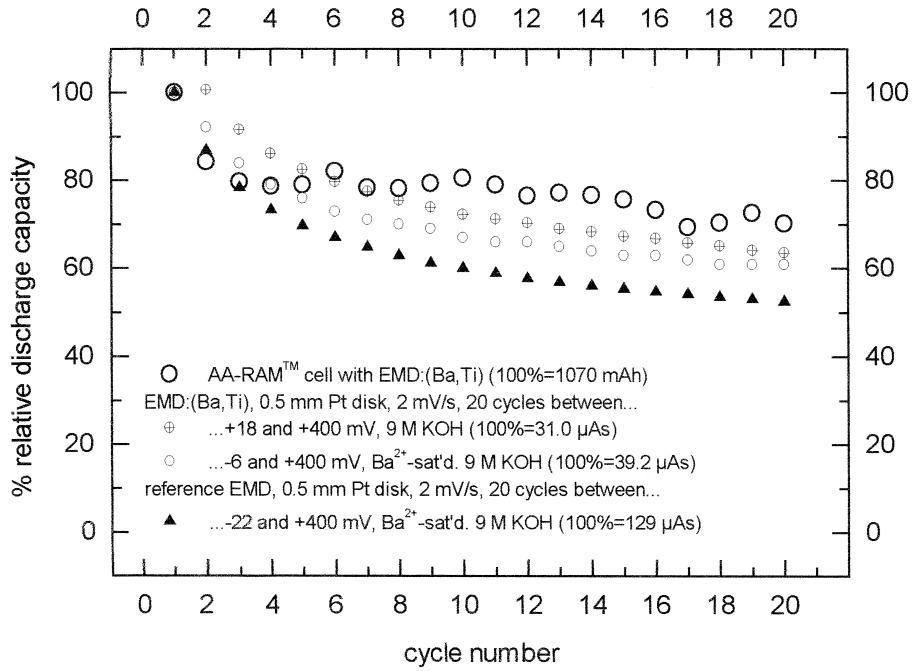

Fig. 10. Relative discharge capacities of reference EMD and EMD (Ba,Ti) under conditions of AbrSV at 30% DOD. Values corresponding to each 100% discharge capacity are shown. Comparison with data for AA-sized cells which were derived from cycles where the cell was discharged across a 3.9 Ω resistor to 900 mV and subsequently voltage-limited taper charged to 1720 mV.

lead to removal of pore-blocking carbonate, which, due to unfavourable solubility equilibrium conditions, is hardly possible in the presence of Ba^{2+}-saturated KOH. Relative discharge capacities at 30% DOD of EMD:Ba are well-comparable to those of reference EMD in barium-saturated 9 M KOH, Fig. 9. These findings support the previously discussed similarity of reference EMD and EMD:Ba, namely BET surface area, powder appearance and cyclic AbrSV response.

When comparing the relative discharge capacities of AA-sized cells containing EMD:Ba with that of multiple voltammetric cycling, the previously reported applicability of AbrSV to the rapid evaluation of EMDs for the use in real cells [9] is strongly supported. This comparison is understood to be qualitative since AbrSV cycling of γ-MnO_2 represents conditions of high-rate 30% discharge, while that of AA cells is a medium- to low-rate 50% discharge [18]. AA cells are conventionally discharged across a constant ohmic load ($R = 3.9\ \Omega$) to 900 mV and subsequently charged by the voltage-limited taper charging method to 1720 mV cell voltage [17,18]. So, while not showing identical relative discharge capacities, which is due to the differing modes of discharge, the same trend of data can certainly be observed from about 15 discharge/charge cycles onwards.

Quite similar to EMD:Ba, data of EMD:(Ba, Ti) in either plain or barium-saturated 9 M KOH does not differ to a significant extent (Fig. 10). However, other than EMD:Ba, EMD:(Ba, Ti) represents higher and more stable relative discharge capacity values than reference EMD in Ba^{2+}-containing KOH under conditions of AbrSV. Relative discharge capacity values from AA-sized cells whose cathodes were made from EMD:(Ba, Ti) this time show both the same trend and quite similar values as those from AbrSV. Clearly, absolute capacities of AA-sized RAM™ cells which contain EMD:(Ba, Ti) are well-comparable to those made from undoped EMD (cf. Fig. 9). We think that the higher internal resistance of EMD:(Ba, Ti) is offset by the usually applied graphite content of about 5–10 wt.% in the cathode [17].

4. Conclusions

Barium- and barium-/titanium-doped EMDs were prepared on the laboratory scale. Barium-doped EMD was found to compare well to commercially available material with respect to microscopic appearance and BET surface area. However, Ba-/Ti-doped EMD exhibited a fourfold increase in BET surface area and an increased internal resistance as deduced from voltammetric experiments. Abrasive stripping voltammetry has been confirmed to be a valuable method in the field of battery electrode material research. Only tens of minutes are necessary to obtain the same information as regards rechargeability when applying AbrSV. Data trends from multiple cycling experiments under conditions of AbrSV appear to be directly comparable to those derived from the conventional testing of AA-sized rechargeable alkaline manganese dioxide cells. This could particularly be shown for a newly synthesized

titanium-doped EMD. This material exhibits superior charge retention and rechargeability when compared to undoped EMDs.

Acknowledgements

D.A. Fiedler thanks the Austrian 'Fonds zur Förderung der wissenschaftlichen Forschung' for support under Lise-Meitner project no. M 00383-CHE. The authors are indebted to Dr. K. Reichmann for recording the SEM images. TEM investigations were performed by I. Papst at 'Forschungsinstitut für Elektronenmikroskopie und Feinstrukturforschung' of Technische Universität Graz. Inductively coupled plasma analyses were thankfully carried out by M. Zischka of 'Institut für Analytische Chemie' of Technische Universität Graz. Batteries were prepared and tested by S. Šimić.

References

[1] H.S. Wroblowa, in: O.J. Murphy, S. Srinivasan, B.E. Conway (Eds.), Electrochemistry in Transition, Plenum, New York, 1992, p. 147.
[2] K.V. Kordesch, J. Gsellmann, Ger. Pat. DE 33 37 568 C2, 1989.
[3] L. Binder, W. Jantscher, D.A. Fiedler, K.V. Kordesch, in: C.F. Holmes, A.R. Landgrebe (Eds.), Batteries for Portable Applications and Electric Vehicles, PV 97-18, The Electrochemical Society, Orlando, 1997, p. 583.
[4] F. Scholz, L. Nitschke, G. Henrion, Naturwissenschaften 76 (1989) 71.
[5] F. Scholz, L. Nitschke, G. Henrion, F. Damaschun, Fresenius Z. Anal. Chem. 335 (1989) 189.
[6] F. Scholz, B. Lange, Trends Anal. Chem. 11 (1992) 359.
[7] F. Scholz, B. Lange, Chem. Soc. Rev. 23 (1994) 341.
[8] D.A. Fiedler, J.O. Besenhard, M.H. Fooken, J. Power Sources 69 (1997) 157.
[9] D.A. Fiedler, J. Solid State Electrochem., 1998, in press.
[10] D.A. Fiedler, J.O. Besenhard, in: C.F. Holmes, A.R. Landgrebe (Eds.), Batteries for Portable Applications and Electric Vehicles, PV 97-18, The Electrochemical Society, Orlando, 1997, p. 893.
[11] O.L. Krivanek, A.J. Gubbens, N. Dellby, C.E. Meyer, Microsc. Microanal. Microstruct. 3 (1992) 187.
[12] F. Hofer, P. Warbichler, W. Grogger, Ultramicroscopy 59 (1995) 15.
[13] H. Tamura, K. Ishizeki, M. Nagayama, R. Furuichi, J. Electrochem. Soc. 141 (1994) 2035.
[14] J. McBreen, Power Sources 5 (1975) 525.
[15] J. McBreen, Electrochim. Acta 20 (1975) 221.
[16] J. McBreen, in: A. Kozawa, R.J. Brodd (Eds.), Manganese Dioxide Symposium, The Electrochemical Society, Vol. 1, Cleveland, 1975, p. 97.
[17] K. Kordesch, K. Tomantschger, J. Daniel-Ivad, in: D. Linden (Ed.), Handbook of Batteries, McGraw-Hill, New York, 1995, p. 34.1.
[18] K. Kordesch, M. Weissenbacher, J. Power Sources 51 (1994) 61.
[19] J.H. Albering, M. Weissenbacher, K. Reichmann, J.O. Besenhard, K. Kordesch, Z. Kristallogr. 9 (1995) 56.
[20] D.A. Fiedler, J.H. Albering, J.O. Besenhard, K. Kordesch, J. Solid State Electrochem., 1998, manuscript in preparation.
[21] J.H. Albering, D.A. Fiedler, J.O. Besenhard, K. Kordesch, J. Solid State Electrochem., 1998, manuscript in preparation.
[22] A. Kozawa, in: K.V. Kordesch (Ed.), Batteries, Manganese Dioxide, Vol. 1, Marcel Dekker, New York, 1974, p. 385.